Effect of inorganic anions on the morphology and structure of magnesium calcite

ARTICLE *in* CHEMISTRY - A EUROPEAN JOURNAL · JANUARY 2004

Impact Factor: 5.73

5 AUTHORS, INCLUDING:

Damir Kralj
Ruđer Bošković Institute
57 PUBLICATIONS **1,049** CITATIONS
SEE PROFILE

Vesna Noethig-Laslo
Ruđer Bošković Institute
58 PUBLICATIONS **375** CITATIONS
SEE PROFILE

Effect of Inorganic Anions on the Morphology and Structure of Magnesium Calcite

Damir Kralj,*[a] Jasminka Kontrec,[a] Ljerka Brečević,[a] Giuseppe Falini,[b] and Vesna Nöthig-Laslo[c]

Abstract: Calcium carbonate was precipitated from calcium hydroxide and carbonic acid solutions at 25 °C, with and without addition of different magnesium ($MgSO_4$, $Mg(NO_3)_2$ and $MgCl_2$) and sodium salts (Na_2SO_4, $NaNO_3$ and NaCl) of identical anions, in order to study the mode of incorporation of magnesium and inorganic anions and their effect on the morphology of calcite crystals over a range of initial reactant concentrations and limited $c_i(Mg^{2+})/c_i(Ca^{2+})$ molar ratios. The morphology, crystal size distribution, composition, structure, and specific surface area of the precipitated crystals, as well as the mode of cation and anion incorporation into the calcite crystal lattice, were studied by a combination of optical and scanning electron microscopy (SEM), electronic counting, a multiple BET method, thermogravimetry, FT-IR spectroscopy, X-ray diffraction (XRD), and electron paramagnetic resonance (EPR) spectroscopy. In the systems of high initial relative supersaturation, precipitation of an amorphous precursor phase preceded the formation of calcite, whereas in those of lower supersaturation calcite was the first and only polymorphic modification of calcium carbonate that appeared in the system. The magnesium content in calcite increased with the magnesium concentration in solution and was correlated with the type of magnesium salt used. Mg incorporation caused the formation of crystals elongated along the calcite *c* axis and, in some cases, the appearance of new {011} faces. Polycrystalline aggregates were formed when the $c_i(Mg^{2+})/c_i(Ca^{2+})$ molar ratios in solution were increased. Addition of sulfate ions, alone, caused formation of spherical calcite polycrystalline aggregates.

Keywords: anions · calcite · crystal growth · crystal morphology · magnesium

Introduction

Calcium carbonate is one of the most important raw materials for use as a filler and pigment in the production of paper, plastics, rubber, paint, textiles, pharmaceuticals, food, and many other materials. Such a variety of applications requires it to have different granulometric, physical and chemical properties. Both natural (limestone, marble, chalk and coral) and synthetic (precipitated) calcium carbonates are commonly used. Natural ground calcium carbonate (GCC), obtained by mechanical treatment of minerals, often does not meet the market demands for the high quality of a product. To meet these needs, calcium carbonate should be prepared under carefully controlled conditions. Only precipitated calcium carbonate (PCC) can provide a product with the characteristics required, as it is precipitated in three anhydrous polymorphic modifications (calcite, aragonite and vaterite), two hydrated crystalline forms (calcium carbonate monohydrate–monohydrocalcite and calcium carbonate hexahydrate–ikaite) and amorphous calcium carbonate,[1,2] which provide plenty of possibilities of yielding a product with predetermined properties. In contrast, calcium carbonate produced from minerals is mostly calcite. The most often used technological PCC production process is the recarbonation of milk of lime.[3,4] The properties of PCC produced in such a process are influenced principally by temperature and the presence of suspended $Ca(OH)_2$ particles.

[a] Dr. Sc. D. Kralj, Dr. Sc. J. Kontrec, Dr. Sc. L. Brečević
Laboratory for Precipitation Processes
Division of Materials Chemistry
Ruđer Bošković Institute
P.O. Box 180, HR-10002 Zagreb (Croatia)
Fax: (+385) 1-4680-098
E-mail: kralj@rudjer.irb.hr

[b] Dr. G. Falini
Dipartimento di Chimica "G. Ciamician"
Università degli Studi
via Selmi 2, 40126 Bologna (Italy)

[c] Dr. Sc. V. Nöthig-Laslo
Laboratory for Magnetic Resonance
Division of Physical Chemistry
Ruđer Bošković Institute
P.O. Box 180, HR-10002 Zagreb (Croatia)

 DOI: 10.1002/chem.200305313

Deposition of calcium carbonate in biological systems occurs during the formation of mollusc shells, egg shells, exoskeletons of arthropods, pearls, and corals.[5] In all these mineralized tissues an organic matrix plays an important role in control of the orientation, polymorphism, composition, and morphology of the mineral phase.

Many studies have been carried out on the mechanisms involved in biomineralization processes and several new biologically inspired synthetic routes have been designed for control of the formation of the mineral phase.[6–8] It has been shown that the polymorphism, morphology and structural properties of calcium carbonate can be controlled by the use of specific additives, macromolecules, small organic molecules and inorganic ions.[9–16] Among the inorganic components, magnesium has a particularly important role in calcium carbonate precipitation. Under certain thermodynamic conditions, magnesium can act either as a very effective inhibitor of nucleation and/or crystal growth of calcite or as a promoter of aragonite nucleation. The inhibition of calcite formation could be explained by the possible preferential adsorption of strongly hydrated magnesium ions onto the growing calcite surfaces, or by enhancement of the calcite solubility caused by incorporation of magnesium into the calcite structure.[11,12] The role of magnesium as a promoter of aragonite formation is closely related to its ability to inhibit calcite nucleation.[17] When the conditions are such that the formation of calcite nuclei is significantly reduced, the nucleation of the less stable polymorph, aragonite, can take place.

Our purpose in this paper is to investigate the influence of factors, other than those connected with the suspension characteristics and temperature, on the physical and chemical properties of precipitated calcium carbonate. Primarily, this is a systematic study of the influence of foreign ions (common anions and Mg^{2+}), the possible impurities in a precipitation system. Therefore, calcium carbonate polymorphs were precipitated from a homogeneous system in which calcium hydroxide and carbonic acid were the reactants. In this case, any possible effects of ions other than the constituents (Ca^{2+}, CO_3^{2-}) and the products of autoprotolysis of water (H_3O^+, OH^-) on the precipitation of polymorphs have been avoided, and $CaCO_3$ and H_2O are the only products of the reaction. The precipitation diagram was constructed from the data obtained by systematic variations of the reactant concentrations. The information thus obtained were used to find out: a) how the foreign ions added, both cation (Mg^{2+}) and anions (SO_4^{2-}, NO_3^- and Cl^-), affect the morphology of calcite; b) whether these ions are incorporated in the crystal lattice of calcite, and if so, the extent and mode of their incorporation; and c) whether there is any interaction between the cation and the anions in the process of incorporation.

To obtain an insight into how Mg^{2+} and the anions examined affect the unit cell parameters and the local environment of Ca^{2+} in the calcite crystal lattice, apart from X-ray powder diffraction (XRD) and FT-IR spectroscopy, we also used electron paramagnetic resonance (EPR) spectroscopy. The Mn^{2+} paramagnetic ion is the most useful ion for such a study because it is readily substituted for Ca^{2+} in the calcite structure and gives a strong EPR signal at room temperature with a rich information content even in the powder state.[18–24] Qualitative interpretation of the spectral parameters as proposed by Angus et al.[19] was used.

Abstract in Croatian: *Proučavan je način ugradnje magnezija i anorganskih aniona, kao i njihov učinak na morfologiju kristala kalcita. U tu je svrhu kalcijev karbonat taložen iz otopina kalcijeva hidroksida i ugljične kiseline pri 25 °C, uz dodatak i bez dodatka različitih magnezijevih ($MgSO_4$, $Mg(NO_3)_2$ i $MgCl_2$) i natrijevih (Na_2SO_4, $NaNO_3$ i NaCl) soli identičnih aniona. Taloženje je proučavano u određenom području početnih koncentracija reaktanata i unutar ograničenih molarnih omjera $c_i(Mg^{2+})/c_i(Ca^{2+})$. Morfologija, raspodjela kristala po veličini, sastav, struktura i specifična površina istaloženih kristala, kao i način ugradnje kationa i aniona u kristalnu rešetku kalcita, proučavani su primjenom optičke i pretražne elektronske mikroskopije (SEM), elektroničkog uređaja za brojanje čestica, BET metode, termogravimetrije, FT-IR spektroskopije, röntgenske difrakcije i elektronske paramagnetske rezonancijske (EPR) spektroskopije. Sadržaj magnezija u kalcitu rastao je s porastom koncentracije magnezija u otopini i pokazao je očitu međuovisnost s tipom upotrijebljene magnezijeve soli. Nađeno je, da u sustavima visoke početne relativne prezasićenosti taloženju kalcita prethodi nastajanje amorfne prekursorske faze, dok se u sustavima nižih prezasićenosti kalcit pojavljuje kao prva i jedina polimorfna modifikacija kalcijeva karbonata. Ugradnja magnezija uzrokovala je nastajanje kristala kalcita izduženih uzduž osi c i, u nekim slučajevima, pojavu novih {011} ploha. S porastom molarnog omjera $c_i(Mg^{2+})/c_i(Ca^{2+})$ u otopini, došlo je do stvaranja polikristalnih agregata, dok je dodatak sulfatnih iona, bez dodatka magnezija, uzrokovao nastajanje polikristalnih agregata kuglastog oblika.*

Results

Precipitation of calcium carbonates: The precipitation was investigated over a range of initial reactant concentrations $c_i(Ca^{2+}) = 0.005–0.010\ mol\,dm^{-3}$ and $c_i(CO_3^{2-}) = 0.001–0.010\ mol\,dm^{-3}$ at 25 °C.

In the three-dimensional precipitation diagram in Figure 1a, two axes represent the total initial concentrations of two variable reactant components, $c_i(Ca)_{tot}$ and $c_i(CO_3)_{tot}$, and the third axis gives the corresponding initial supersaturations over the calcium carbonate precipitation range examined in this work. The initial supersaturation is defined as relative supersaturation, $S-1$, $S = (\prod/K_{sp}^\circ)^{1/2}$, where $\prod$ is the ion activity product $a(Ca^{2+})\cdot a(CO_3^{2-})$, and K_{sp}° is the thermodynamic equilibrium constant of dissolution of the most stable calcium carbonate polymorph, calcite ($K_{sp}^\circ = 3.313\times10^{-9}$ at 25 °C). From the known total concentrations of $Ca(OH)_2$ and H_2CO_3 initially added to the precipitation system, the molar concentrations and the corresponding activities of all relevant ionic species that were assumed to exist at considerable concentrations in the solution (H^+,

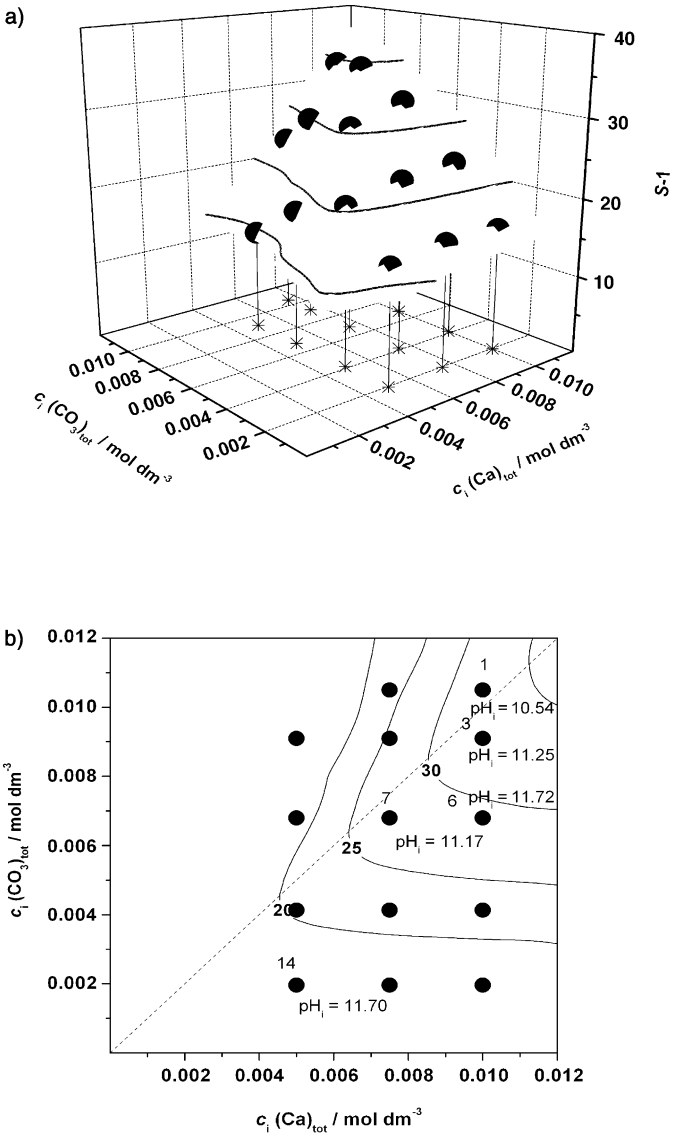

Figure 1. a) Three-dimensional precipitation diagram of the system $Ca(OH)_2$–H_2CO_3–H_2O; b) its projection on the *x*–*y* plane. Aging time 20 min, 25 °C. For details, see the main text.

OH^-, CO_3^{2-}, HCO_3^-, $CaCO_3^0$, $CaHCO_3^+$, Ca^{2+}, $CaOH^+$) were calculated. The detailed calculation procedure, which takes into account the respective protolytic equilibria and equilibrium constants as well as the charge- and mass-balance equations, has been described previously.[25–27]

Isergons (isograms for constant supersaturation) are indicated; the samples selected for detailed analyses are denoted by solid circles. The projection on the x–*y* plane of the precipitation region from Figure 1a is shown in Figure 1b. The initial pH of the reactant solutions was not preadjusted to a certain value: the calculated initial pH for each ratio of the initial total concentration of calcium and carbonate is shown in Figure 1b alongside the solid circle representing the relevant sample.

Additional consideration was given to the samples with the greatest amount of solid precipitated (samples 1, 3, 6, and 7 in Figure 1b), that is, to the samples obtained from the systems with reactant concentrations close to equimolar. The solid phase of these samples, aged for 20 min after the reactants were mixed, was mostly calcite; only samples 1 and 3 also contained vaterite. This is not surprising, since the formation of metastable phases during spontaneous precipitation from highly supersaturated solutions is quite common. Besides, immediately after the mixing of the reactant solutions, very high turbidity and a simultaneous drop in pH were noticed, indicating the formation of an amorphous precursor.[1,28–30] Although the primary intention in this work was not to study this precursor phase, its possible impact on the physical and chemical properties (for example, morphology, composition of precipitate) of the more stable solid phases (calcite, magnesium calcite, aragonite) and on later stages of the precipitation process had to be examined.[2,31,32] Therefore, the change in pH was recorded and several samples were taken from the precipitation system during the first 20 min of the process and then analyzed. The experimental steplike curve of pH versus time (Figure 2A) which was recorded during the precipitation of

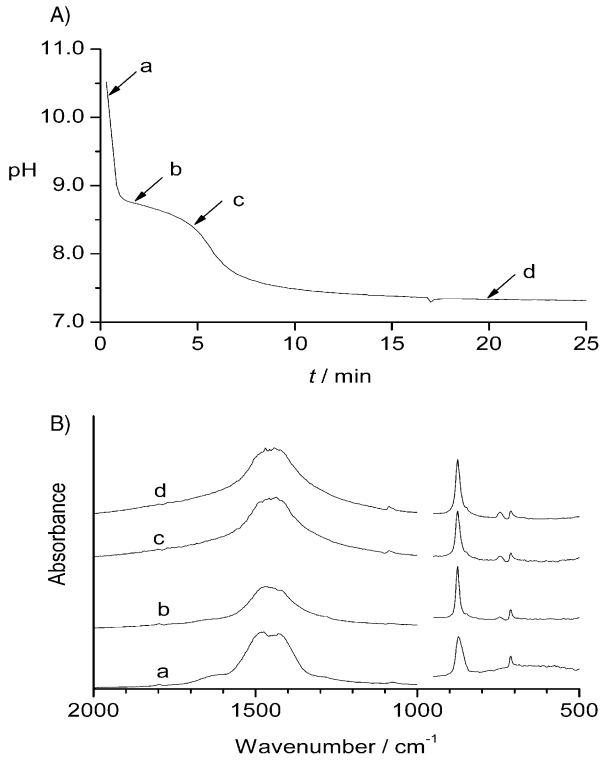

Figure 2. A) Changes in pH as a function of time during precipitation of sample 1 (Figure 1); B) FT-IR spectra of precipitates isolated at time intervals a–d as indicated on the pH curve.

sample 1 (Figure 1b) is typical of the precipitation processes in which the initial formation of metastable (precursor) phase(s) is followed by a recrystallization process that takes place through the so-called solution-mediated transformation.[25,29] FT-IR spectra (Figure 2B) of the samples isolated from the system at time intervals a–d (see Figure 2A) support the assumption that an amorphous phase appears in the early stage of the process. This amorphous phase was identi-

fied by means of the absorption bands characteristic of amorphous calcium carbonate.[2,30] Spectrum a, obtained from the sample isolated within 1 min after mixing the reactants, exhibits the characteristic bands at about 1490 and 1430 cm^{-1} (ν_{3a}, ν_{3b}), 1080 cm^{-1} (ν_1) and 866 cm^{-1} (ν_2). The bands at 725 and 690 cm^{-1} (ν_{4a}, ν_{4b}) are broadened extensively, so that no discrete peaks could be observed. The bands at 1640 cm^{-1}, corresponding to the normal vibration of water molecules (H–O–H bending) in the structure of amorphous calcium carbonate, are also exhibited. Calcite in this sample was identified by the absorption bands at 713 and 876 cm^{-1} (ν_4 and ν_2, respectively); the calcite content was estimated, from the known value of the molar absorption coefficient for calcite at 713 cm^{-1}, to be approximately 15 %.[33] Spectrum b, obtained from the precipitate separated about 2 min after the mixing of the reactants, exhibits the absorption bands characteristic of vaterite (746 cm^{-1}, ν_4), apart from the absorption bands characteristic of calcite; this spectrum still contains traces of amorphous calcium carbonate bands. At that stage of precipitation, the precursor phase was in a process of transformation into vaterite and/or calcite. The sample isolated at the end of the discontinuous drop in pH is represented by spectrum c, which exhibits bands characteristic of vaterite and calcite only. The amorphous precursor had disappeared from the system by that time, as evidenced also by a reduction in turbidity. The second drop in pH, which follows the discontinuity, indicates the crystal growth of stable phase(s). Thus, spectrum d exhibits the absorption bands of calcite and vaterite. A spectrum of the sample separated 24 h after preparation of the system (not shown here) exhibited only the characteristics of the thermodynamically stable polymorph calcite, as the vaterite previously present in the system had been transformed into calcite in the meantime. It should be emphasized that some recent investigations[2,34] gave experimental evidence showing that the term "amorphous calcium carbonate" describes two groups of phases: a hydrated modification, containing up to one water molecule per mole of calcium carbonate; and an (essentially) anhydrous modification. Apart from the structural differences and different degrees of ordering, these two groups differ in their mechanism of transformation into the (more) stable polymorphs. Transformation of anhydrous amorphous calcium carbonate takes place through an internal reorganization ("solid-state transformation") leading to the crystalline structure of a stable form, either calcite or aragonite. Transformation of the hydrated modifications is the "solution-mediated process", that is, simultaneous dissolution of amorphous calcium carbonate and nucleation and growth of stable modification(s). Accordingly, the amorphous precursor detected in this work may have been a hydrated modification of the amorphous calcium carbonate.

FT-IR spectra of all the other samples denoted in Figure 1, isolated from the systems 20 min after the mixing of the reactants, showed either the absorption bands characteristic of calcite or the bands of calcite and vaterite. The specific surface area of the samples containing both calcite and vaterite was 3.7 $m^2 g^{-1}$, and that of the samples with calcite as the only solid phase was in the range 0.7–1.6 $m^2 g^{-1}$. The difference between these two groups of samples is quite noticeable. The reason for such a difference lies not only in the different sizes of the calcite crystals, as is the case for samples consisting of calcite only, but also in the presence of vaterite particles. These are usually spherulites with an irregular, rough surface, the specific surface area of which can be an order of magnitude larger than the specific surface area of the compact calcite crystals.[25,35] Although these samples contain a relatively small amount of vaterite particles, its contribution to the specific surface area of the sample as a whole is quite evident. Figure 3 shows some typical number distributions of the samples examined. Those consisting of calcite and vaterite (samples 1 and 3) exhibited a maximum at about 14 μm ascribed to the quite uniform, compact calcite crystals, and a wide range of smaller crystal sizes (< 10 μm) related to the spherulitic vaterite particles. Such a wide range of vaterite particle sizes suggests that the vaterite was in the process of transformation into calcite. As reported previously,[25] this process is solution-mediated, which means that calcite crystals grow on account of vaterite particle dissolution. The wider crystal size distributions were also obtained for the samples (such as sample 6) that precipitated at somewhat lower initial supersaturations ($25 < (S-1) < 30$). The majority of calcite crystals in these samples were about 7–11 μm in size. The presence of some smaller crystals (< 6 μm) in the samples suggests that crystal growth was in progress when the process was interrupted, 20 min after the mixing of the reactants. In contrast to the samples precipitated at relatively high supersaturations, the precipitation initiated at lower supersaturations ($(S-1) < 20$) clearly proceeds by another mechanism. There was no precursor phase formation, the number of calcite crystals was smaller and the crystals grew comparatively slowly. At such supersaturations, the decrease in pH in the system was very slow and continuous with a simultaneous gradual increase in turbidity. The reaction was preceded by a visually observed induction period. All this corroborates the assumption that heterogeneous nucleation with slow crystal growth is the mechanism of precipitation at lower supersaturations. In this way, a very narrow distribution of small crystals (maximum at about 4 μm) was obtained (sample 14).

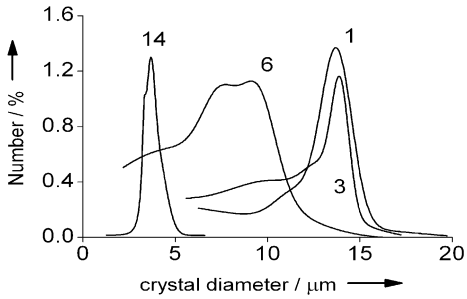

Figure 3. Crystal size distributions for samples 1, 3, 6 and 14 (numbered as in Figure 1b) obtained 20 min after mixing the reactant solutions. They were measured with the electronic counting device (Coulter Electronics Ltd) and given in differential mode.

A systematic investigation of the influence of magnesium on the physical-chemical properties of the precipitated calcium carbonate was performed for the ranges of $c_i(Ca^{2+})$ and $c_i(CO_3^{2-})$ identical to those shown in Figure 1. For this purpose, the second cationic component, Mg^{2+}, was added to the systems and the initial molar ratio $c_i(Mg^{2+})/c_i(Ca^{2+})$ was kept at 1:1 in one case and 1:2 in the other. These relatively low $c_i(Mg^{2+})/c_i(Ca^{2+})$ molar ratios were chosen so as to be comparable with the values found in natural and technological systems, and also to avoid the precipitation of aragonite.[9,36] No matter which of the three magnesium salts ($MgCl_2$, $Mg(NO_3)_2$ or $MgSO_4$) was used, in addition to calcite the coprecipitation of some amorphous $Mg(OH)_2$ was observed over the entire precipitation region examined, except when there was an excess of CO_3^{2-} ions and at the lowest supersaturations ($(S-1)<20$). Aragonite also appeared in some of the systems with molar ratio $c_i(Mg^{2+})/c_i(Ca^{2+}) = 1:1$, as a consequence of kinetic inhibition of calcite nucleation and growth[37] rather than of thermodynamic factors.

Isomorphic substitution of magnesium ions in the calcite structure: For the reasons mentioned above (coprecipitation of amorphous $Mg(OH)_2$, precipitation of some vaterite or aragonite), the influence of the initial $c_i(Mg^{2+})/c_i(Ca^{2+})$ ratio, and of the type of co-anion present in the system during precipitation, on the extent and mode of magnesium incorporation into the calcite lattice was investigated exclusively in the system in which the total initial reactant concentrations were $c_i(Ca^{2+}) = 0.005\ mol\,dm^{-3}$ and $c_i(CO_3^{2-}) = 0.010\ mol\,dm^{-3}$. This system was chosen following the calculations in which a literature value of the thermodynamic solubility product of brucite, $Mg(OH)_2$, ($pK_{sp}^{\circ} = 11.15$) was used. From the data obtained it may be concluded that coprecipitation of $Mg(OH)_2$ is not possible at $pH \leq 9.45$ and at the initial concentration of Mg^{2+} ($c_i = 0.010\ mol\,dm^{-3}$) applied in these experiments. Indeed, in this system, the measured initial pH_i was 9.3, no $Mg(OH)_2$ was coprecipitated and no other Mg solid phase was detected, and calcite was the first and only crystal modification appearing. Magnesium was added to the system in the form of $MgCl_2$, $Mg(NO_3)_2$ or $MgSO_4$, in such concentrations that the initial ratio $c_i(Mg^{2+})/c_i(Ca^{2+}) = 0.5:1$, 1:1 or 2:1. Changes in the unit cell volume of calcite precipitated in the presence of magnesium and, based on these data, the number percentages of magnesium atoms incorporated in the calcite crystal lattice, were determined by XRD of powdered samples. The calcite unit cell parameters as a function of the initial Mg^{2+}/Ca^{2+} molar ratio and the percentage of magnesium atoms incorporated in calcite in the presence of different inorganic ions are given in Table 1. The magnesium content in the samples was also analyzed by ion chromatography. Figure 4 shows the relationships between magnesium substitution in calcite and the initial $c_i(Mg^{2+})/c_i(Ca^{2+})$ ratio. The magnesium substitution was found to depend on the type of magnesium salt used. Thus, the greatest magnesium content in calcite was recorded when $MgSO_4$ was used, followed by $Mg(NO_3)_2$ and then $MgCl_2$. These contents were still much lower than those when $Mg(OH)_2$ served as the magnesium source (control system). The highest initial concentration of magnesium in the systems in which $Mg(OH)_2$ was used as the magnesium source was $0.005\ mol\,dm^{-3}$ (initial molar ratio $c_i(Mg^{2+})/c_i(Ca^{2+}) = 1:1$). Any higher concentrations of $Mg(OH)_2$ led to an increase in pH and, consequently, to the coprecipitation of $Mg(OH)_2$. From the experimental evidence, the process and the extent of magnesium incorporation in the calcite lattice probably depend very much on the Mg-accompanying anions. These findings justify our precautions in choosing the appropriate precipitation components, that is, bringing about the precipitation of calcium carbonate by mixing $Ca(OH)_2$ and H_2CO_3 solutions. In this way, no other anions except CO_3^{2-}/HCO_3^- and OH^- could influence the physical-chemical properties of the precipitate. This could also explain a rather large amount of magnesium de-

Table 1. Calcite unit cell parameters as a function of the initial Mg^{2+}/Ca^{2+} molar ratio in solutions containing different inorganic anions.

Additive	Mg/Ca [mol mol^{-1}]	Calcite unit cell parameters a [nm]	c [nm]	V [nm]	Mg [atom %][a]
$MgCl_2$	0.5:1	0.4956	1.7348	369.032	–
$Mg(NO_3)_2$	0.5:1	0.4952	1.7376	369.043	–
$Mg(SO_4)_2$	0.5:1	0.4949	1.7370	368.496	–
$Mg(OH)_2$	0.5:1	0.4926	1.7186	361.122	6.5(7)
$MgCl_2$	1:1	0.4954	1.7207	364.443	3.1(5)
$Mg(NO_3)_2$	1:1	0.4949	1.7317	367.322	5.1(6)
$Mg(SO_4)_2$	1:1	0.4935	1.7282	364.521	6.3(5)
$Mg(OH)_2$	1:1	0.4910	1.7186	361.122	8.1(6)
$MgCl_2$	2:1	0.4929	1.7276	363.733	3.8(7)
$Mg(NO_3)_2$	2:1	0.4926	1.7198	361.380	6.5(7)
$Mg(SO_4)_2$	2:1	0.4917	1.7188	359.847	7.5(7)

[a] Obtained by volume contraction.[38]

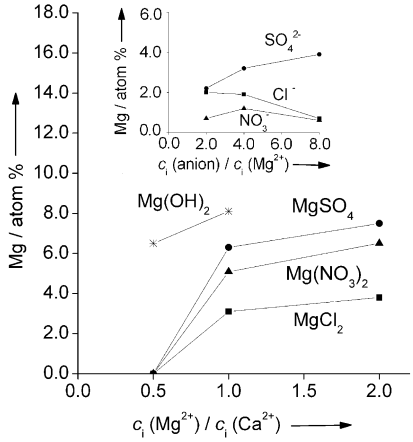

Figure 4. Magnesium content [atom %] in the calcite samples as a function of the initial molar ratio $c_i(Mg^{2+})/c_i(Ca^{2+})$. The samples were obtained from the system $c_i(Ca^{2+}) = 0.005\ mol\,dm^{-3}$, $c_i(CO_3^{2-}) = 0.010\ mol\,dm^{-3}$, 20 min after mixing the reactants, at different initial concentrations of Mg^{2+} and from diverse sources, at 25 °C. Inset: magnesium content [atom %] as a function of the initial molar ratio $c_i(anion)/c_i(Mg^{2+})$ in the system $c_i(Ca^{2+}) = 0.005\ mol\,dm^{-3}$, $c_i(CO_3^{2-}) = 0.01\ mol\,dm^{-3}$ to which different magnesium salts ($c_i(Mg^{2+})/c_i(Ca^{2+}) = 1:1$) and the appropriate sodium salts were added in order to obtain various initial molar ratios $c_i(anion)/c_i(Mg^{2+})$ under otherwise comparable conditions.

tected in the calcite samples treated with $Mg(OH)_2$, compared with the amounts reported in the literature[9] for similar experimental conditions (in these samples also, no additional anions were present).

Additional experiments were performed to elucidate the role of anions in magnesium incorporation into the calcite lattice. They were carried out under conditions similar to those described previously ($c_i(Ca^{2+}) = 0.005\,mol\,dm^{-3}$, $c_i(CO_3^{2-}) = 0.010\,mol\,dm^{-3}$, initial molar ratio $c_i(Mg^{2+})/c_i(Ca^{2+}) = 1:1$). The only difference was the addition of the respective sodium salt, Na_2SO_4, $NaNO_3$ or NaCl, so that the molar ratio $c_i(Mg^{2+})/c_i(anion) = 1:2$, 1:4 and 1:8, thus exceeding the stoichiometry of the respective Mg salt. The presence of Na^+ was justified, because no observable impact of this ion on the calcium carbonate precipitation was detected for the range of concentrations applied. The inset in Figure 4 shows that the increase in concentration of either NO_3^- or Cl^-, respectively, does not change much, or causes a gradual decrease in incorporation of magnesium atoms into the crystal lattice of calcite. In contrast, the increase in concentration of SO_4^{2-} ions causes an increase in incorporation of magnesium atoms. These observations, together with the effects of higher incorporation of magnesium into the calcite lattice when $MgSO_4$ and $Mg(OH)_2$ were used as the sources of magnesium, are in accordance with the similar findings reported in the literature.[31] It is known that calcites with a high magnesium content can be produced by using organic molecules able to chelate magnesium. Such chelates suppress the hydration of Mg^{2+} ions, thus giving the possibility of producing high-magnesium calcites. The content of magnesium in such calcites can be above 10 mol% (magnesium calcite with a magnesium content of more than 10 mol% is thermodynamically less stable/soluble than aragonite). The tendency of magnesium to form strong ion pairs with SO_4^{2-} ($K_s°(MgSO_4^+) = 169.8$) and OH^- ($K_s°(MgOH^+) = 380.2$) has an effect similar to that of the organic chelators, that is, it causes lowering of the concentration of strongly hydrated Mg^{2+} ions in solution.

The local distortions induced by Mg^{2+} and the anions examined were investigated by EPR analysis. In Figure 5 the EPR spectra of $^{55}Mn^{2+}$-doped calcites, precipitated in the systems into which Mg^{2+} was introduced by dissolution of $Mg(OH)_2$ (spectra a and b) and incorporating different amounts of Mg^{2+} (8.1 and 6.5 atoms%, respectively), are compared with the spectrum of pure calcite (spectrum c). The presence of Mg^{2+} in the calcite lattice is reflected as an increase in the D' parameter from 1.76 mT (spectrum c) to 1.90 mT (spectrum b) and 1.94 mT (spectrum a), and as an extensive line broadening of all hyperfine linewidths: $\Delta W_\parallel$ changed from 0.27 mT to 0.85 mT and 0.9 mT, respectively. Since no other anions except OH^- and CO_3^{2-} were present in the precipitation system, only Mg^{2+} and the possibly bonded water could provoke these distortions. According to FT-IR spectroscopic and differential thermogravimetric (DTG) analyses, no structural water was detected in these samples, so it seems that the distortions were provoked exclusively by incorporation of Mg^{2+}.

The EPR spectra of calcites prepared in the presence of different magnesium salts ($MgSO_4$, spectrum a; $MgCl_2$, spectrum b; $Mg(NO_3)_2$, spectrum c) are shown in Figure 6. These samples had the highest content of added anions in the system: initial molar ratio $Ca^{2+}/Mg^{2+}/anion = 1:1:8$. Although an increase in the axial distortion parameter D' com-

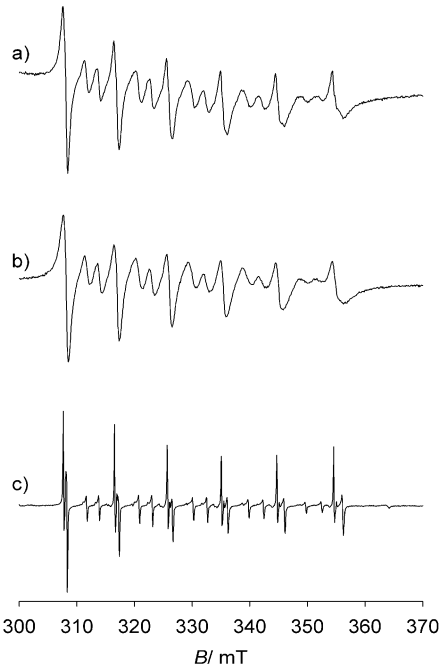

Figure 5. EPR spectra of $^{55}Mn^{2+}$ ($I_{Mn} = 5/2$) in calcites doped with Mg^{2+} from $Mg(OH)_2$ containing [atom% Mg]: a) 8.1; b) 6.5; c) 0. Spectral parameters measured [mT]: a) $D' = 1.94$, $\Delta W_\parallel = 0.9$, $\Delta W_\perp = 2.7$; b) $D' = 1.90$, $\Delta W_\parallel = 0.85$, $\Delta W_\perp = 2.7$; c) $D' = 1.76$, $\Delta W_\parallel = 0.27$, $\Delta W_\perp = 2.7$.

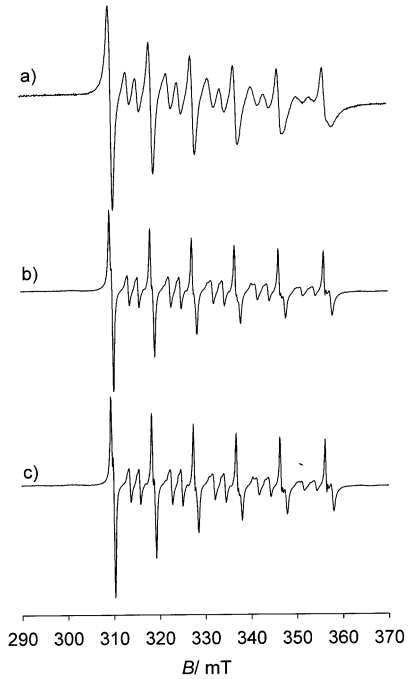

Figure 6. EPR spectra of $^{55}Mn^{2+}$ in calcites prepared in the presence of: a) $MgSO_4$: $D' = 2.02$ mT, $\Delta W_\parallel = 0.92$ mT, $\Delta W_\perp = 1.6$ mT; b) $MgCl_2$: $D' = 1.87$ mT, $\Delta W_\parallel = 0.45$ mT, $\Delta W_\perp = 0.78$ mT; c) $Mg(NO_3)_2$: $D' = 1.88$ mT, $\Delta W_\parallel = 0.35$ mT, $\Delta W_\perp = 0.72$ mT. In each system sampled, initial molar ratio $Ca^{2+}/Mg^{2+}/anion = 1:1:8$.

pared with that of pure calcite (1.76 mT, spectrum c, Figure 5) was observed in spectra b and c, the largest increase in D' concomitant with the extensive line broadening was measured in spectrum a. The disturbances in the calcite crystal lattice observed in the presence of SO_4^{2-} ions were similar to those obtained when calcite was precipitated from the systems in which $Mg(OH)_2$ was used as a magnesium source (see Figure 5). However, the amount of Mg^{2+} incorporated in the presence of SO_4^{2-} ions (3.9 atom %) was much smaller than was incorporated in the presence of $Mg(OH)_2$ (8.1 atom %) and yet the disturbances were larger. DTG and FT-IR spectroscopic analyses detected a small amount of structural water (a loss of approximately 2 wt % at about 290 °C) in calcite prepared with $MgSO_4$. This could cause slightly larger distortions compared with the calcites without any bonded water, but probably not as large as those observed in spectrum a. EPR spectra of the Mn^{2+}-doped calcite precipitated with $Mg(OH)_2$ as the magnesium source reveal the distortions along the axial crystal field as well as the random displacement of the CO_3^{2-} groups about their equilibrium positions. It is evident that, apart from Mg^{2+} and a small amount of structural water found in the sample prepared with the addition of $MgSO_4$, the structure and charge differences between Cl^- or NO_3^- and SO_4^{2-} also have to be considered responsible for the disturbances of the calcite lattice. It seems that SO_4^{2-}, being a tetrahedron, when incorporated to the same extent causes more disturbances of the calcite lattice than (for example) NO_3^-, which has a planar sp^2 hybrid structure similar to that of CO_3^{2-} ions.

Morphological investigations: It is known that ionic additives can considerably affect crystal nucleation and can also adsorb on the crystal surface, often inducing the formation of aggregates.[39,40] Either by inhibiting growth sites of nuclei and thus preventing their growth, or by adsorption on the crystal surface and altering its double-layer surroundings, an increase in the concentration of ionic additive increases the tendency to form aggregates.

Scanning electron micrographs (Figure 7) show the morphologies of calcite crystals formed when $MgSO_4$, $Mg(NO_3)_2$ or $MgCl_2$ was present in the precipitation system $c_i(Ca^{2+}) = 0.005\ mol\,dm^{-3}$ and $c_i(CO_3^{2-}) = 0.010\ mol\,dm^{-3}$ in the molar ratios $c_i(Mg^{2+})/c_i(Ca^{2+}) = 0.5{:}1$, 1:1 and 2:1. When calcite was precipitated in the absence of any additive, the crystals had the well-known rhombohedral shape, characterized by the presence of the most stable {104} faces (see Figure 8a). In the presence of additives, different shapes of calcite crystals were formed as a consequence of additive concentration and anion type. The effect of the anions investigated in this study can be correlated strictly with the content of magnesium added to the solution. As the amount of $MgCl_2$ in solution increases, the crystals show more pronounced development of the {011} faces, which combine with the typical

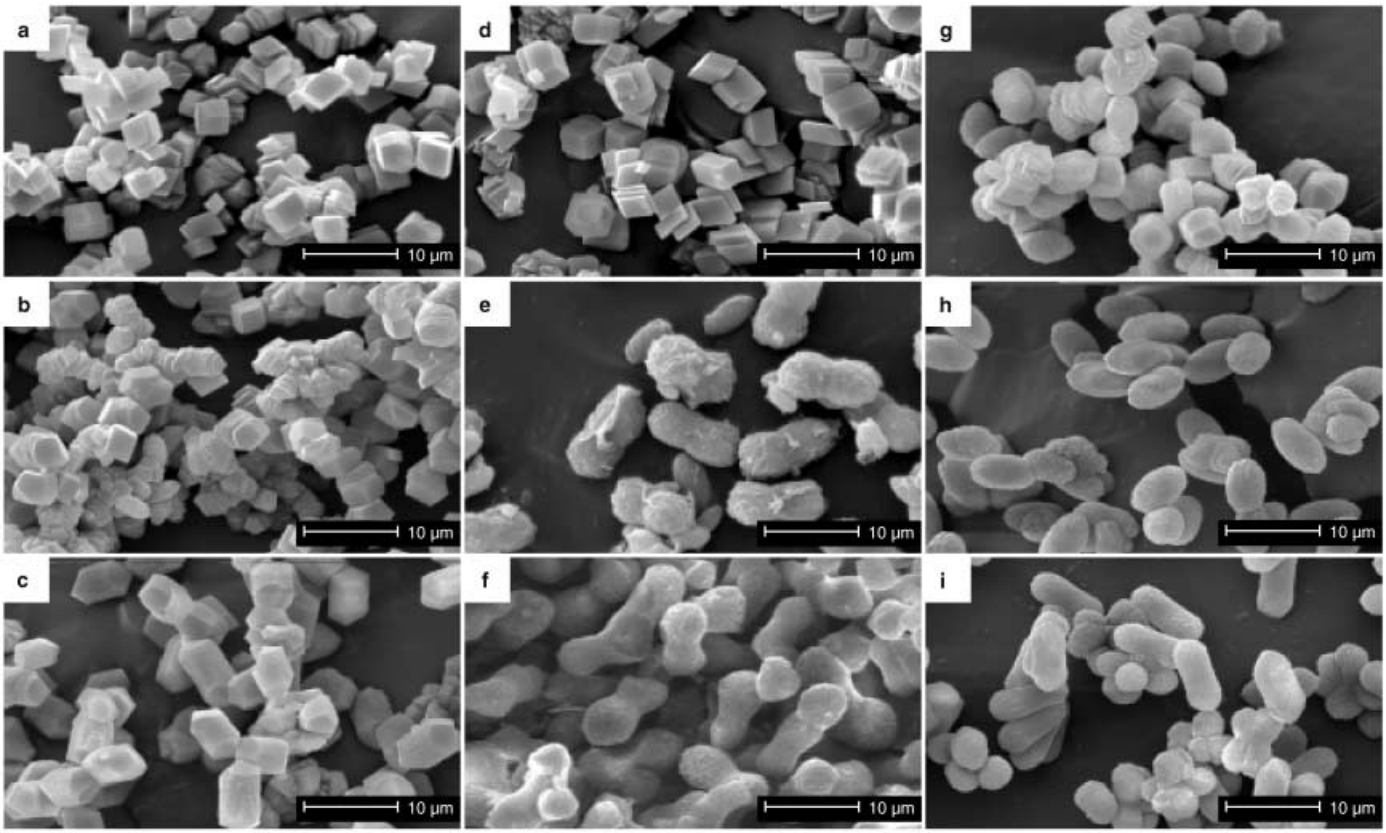

Figure 7. SEM images of calcite crystals isolated from the system $c_i(Ca^{2+}) = 0.005\ mol\,dm^{-3}$, $c_i(CO_3^{2-}) = 0.01\ mol\,dm^{-3}$ at 25 °C, to which the following magnesium salts were added in the initial molar ratios $c_i(Mg^{2+})/c_i(Ca^{2+})$ stated: $MgCl_2$, a) 0.5:1, b) 1:1, c) 1:2; $Mg(NO_3)_2$, d) 0.5:1, e) 1:1, f) 1:2; $MgSO_4$, g) 0.5:1, h) 1:1, i) 1:2.

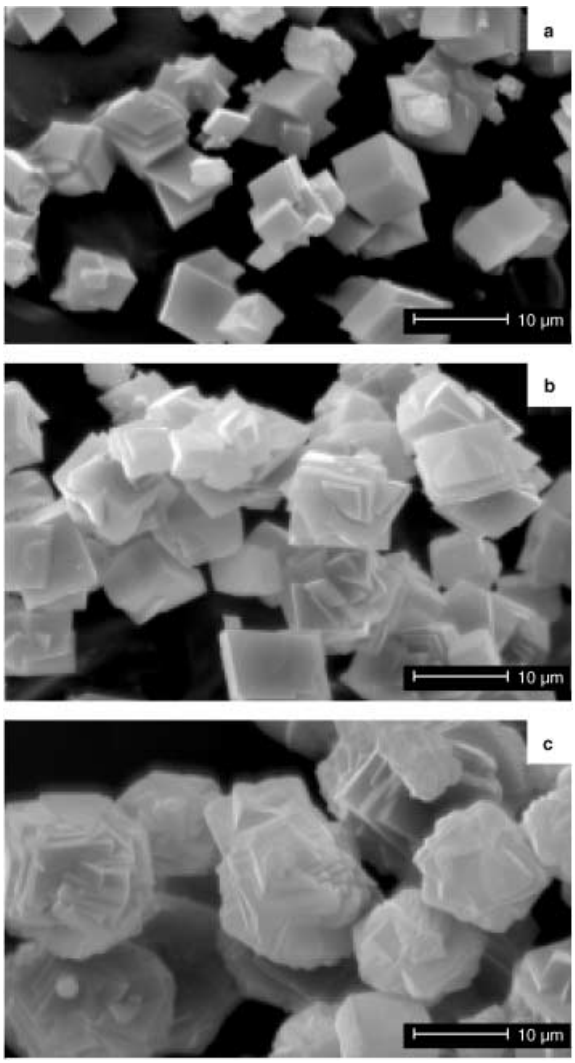

Figure 8. SEM images of a) pure calcite crystals and calcite crystals prepared with an initial molar ratio $c_i(Ca^{2+})/c_i(SO4^{2-})$ of b) 1:0.1 and c) 1:1.5.

rhombohedral {104} calcite faces (Figure 7a–c). As a result of this combination, the crystals become {104} face-capped and elongated along the calcite *c* axis. They always appear as single crystals without any lateral aggregation. The addition of $Mg(NO_3)_2$ to the solution changes the rhombohedral calcite crystals to the dumbbell-shaped crystals[31] at the highest concentration of magnesium applied (Figure 7d–f). These crystals are elongated along the calcite *c* axis but the usual {104} face-capping is not evident. The presence of SO_4^{2-} anions in solution affects the morphology of calcite crystals to a greater extent when compared with chloride ions, which is in agreement with isomorphic substitution data (Figure 7g–i). Even at the lowest content of magnesium relative to calcium in solution ($c_i(Mg^{2+})/c_i(Ca^{2+}) = 0.5:1$), the crystals already show a modified morphology, being elongated along the *c* axis and {104} face-capped. The new faces, almost parallel to the *c* axis, are more stepped than in the case of chloride. The increase in magnesium and sulfate ion concentrations in solution has a dramatic effect on the magnesium calcite morphology. The crystals are no longer {104} face-capped. They are more stepped and seem to be aggregates of small crystalline units elongated along the *c*-axis. The resulting morphology ranges from the intergrown lobes to dumbbells as the amount of additive is increased.[9] To clarify the role of sulfate ions, alone, in affecting the morphology of calcite crystals, increasing concentrations of Na_2SO_4 were added to the system $c_i(Ca^{2+}) = c_i(CO_3^{2-}) = 0.010\ mol\,dm^{-3}$. As an example, Figure 8 shows the morphologies of calcite crystals formed when no additives were applied (Figure 8a) and when the initial ratio $c_i(Ca^{2+})/c_i(SO_4^{2-}) = 1:0.1$ (Figure 8b) and 1:1.5 (Figure 8c). In the presence of sulfate ions the rhombohedral crystals of calcite undoubtedly strive to group themselves in spherical aggregates.

All these findings are in accordance with those reported for modification of rhombohedral calcite crystals when either Mg^{2+} or SO_4^{2-} ions are present in solution, and for the formation of spherical calcite crystals when both Mg^{2+} and SO_4^{2-} ions are present in solution as impurities.[41,42] However, our results reveal that sulfate ions, alone, cause the formation of spherical calcite aggregates. In summary, on the basis of our results, the following conclusions may be drawn about the influence of Mg^{2+} and different anions (SO_4^{2-}, NO_3^- and Cl^-) on the precipitation of calcium carbonate and on the morphology of calcite crystals investigated at 25 °C, in the system in which calcium hydroxide and carbonic acid solutions were used as reactants:

a) In the range of calcium carbonate precipitation examined in this work, calcite is the predominant solid phase formed 20 min after mixing the reactants.
b) At the highest supersaturations, $(S-1) > 30$, the formation of precursor phase(s) (amorphous calcium carbonate) precedes the formation of calcite.
c) The content of magnesium incorporated in the calcite crystals increases with increasing initial concentration of magnesium salt added to the system.
d) The incorporation of magnesium in the calcite crystal lattice depends on the type of co-anion present in the system. For the molar ratios $c_i(Mg^{2+})/c_i(Ca^{2+}) = 1:1$ and 2:1 of the initial solution concentrations, the magnesium content in calcite crystals decreases in the series $MgSO_4 > Mg(NO_3)_2 > MgCl_2$.
e) The highest magnesium content in the calcite lattice can be achieved in systems with no additional anions, such as systems in which the dissolved $Mg(OH)_2$ is used as the magnesium source.
f) Addition of sulfate ions, alone, causes the formation of spherical aggregates of the originally rhombohedral calcite crystals.
g) There is a clear relationship between the morphological properties of magnesium calcites, the concentration of the corresponding anion and the amount of Mg^{2+} incorporated into calcite lattice.
h) EPR measurements of magnesium calcites precipitated from solutions of different anions have revealed different modes and extents of magnesium incorporation. The calcite lattice is the most significantly distorted by the presence of SO_4^{2-}, while Cl^- and NO_3^- have a minor impact.

Experimental Section

A 400 cm^3 double-walled, water-jacketed, thermostated glass crystalliser was used throughout the experiments. Calcium carbonate was precipitated by mixing equal volumes (150 cm^3) of both calcium hydroxide and carbonic acid solutions. The latter solution was prepared by bubbling a high-grade carbon dioxide stream into water until apparent constancy of conductivity or pH was obtained. The exact concentration of this solution was then determined by potentiometric titration using a standard NaOH solution ($c = 0.10\ mol\,dm^{-3}$). The concentrations determined ($c = 0.021\ mol\,dm^{-3}$) of freshly prepared carbonic acid stock solutions were always comparable with those calculated ($c = 0.024\ mol\,dm^{-3}$) from the measured values of $pH_{stock} = 3.99$. Calcium hydroxide stock solution was prepared by adding an excess of analytically pure calcium hydroxide to water. The suspension was then filtered through a 0.22 μm membrane filter and the saturated solution was kept under an atmosphere of nitrogen. The exact concentration was determined by potentiometric titration using the standard HCl solution ($c = 0.10\ mol\,dm^{-3}$). In all the experiments the water was deionized and of high quality (conductivity < 0.1 $\mu S\,cm^{-1}$). The freshly prepared carbonic acid solution of known concentration (diluted from the stock solution), pure or with the required amount of extra salt(s) added (magnesium sulfate, magnesium nitrate, magnesium chloride, sodium sulfate, sodium nitrate and sodium chloride) was always poured into the calcium hydroxide solution. The initial calcium and carbonate reactant concentrations are given in the precipitation diagram (Figure 1).

The effect of sulfate ions on the morphology of calcite crystals was investigated by addition of sodium sulfate to the carbonic acid solution. In this series of experiments the initial ratio $c_i(Ca^{2+})/c_i(SO_4^{2-}) = 1{:}0.1,\ 1{:}0.5,\ 1{:}1.5$, or 1:2.

To study the effect of different Mg salts on the physical-chemical properties of the precipitate, the respective salt ($MgCl_2$, $Mg(NO_3)_2$ or $MgSO_4$) was added to the $Ca(OH)_2$ solution. If not stated otherwise, the initial $c_i(Mg^{2+})/c_i(Ca^{2+})$ ratio was kept at 0.5:1 or 1:1.

When the effect of possible synergistic action of anions on the extent of magnesium incorporation was investigated, a stoichiometric excess of anion (above the stoichiometry of the respective Mg salt) was added to the system in the form of the respective sodium salt (ratio $c_i(Mg^{2+})/c_i$(anion) = 1:2, 1:4 or 1:8). The control system (that is, the system in which no additional anion could influence the incorporation of magnesium into calcite, except CO_3^{2-}/HCO_3^- and OH^-), was prepared by dissolving an appropriate amount of $Mg(OH)_2$ into the carbonic acid solution before mixing with the $Ca(OH)_2$ solution.

During the experiments, the systems were stirred at a constant rate by a flat-bladed stirrer with two perpendicular blades. All experiments were carried out at 25 °C.

The propagation of the reaction was followed by measuring the pH of the solution; the samples were taken after a predetermined aging time of 20 min. When the reaction was stopped, the total volume of suspension was filtered through a 0.22 μm membrane filter and the precipitate was dried at 105 °C.

Crystal number and size distributions were determined with an electronic counting device (Coulter Electronics Ltd.) fitted with a 50 μm-orifice tube. This aperture diameter enabled crystals in the size range between about 1 and 30 μm to be measured and distributed into up to 256 size classes. Each class corresponds to a nominal crystal diameter, that is, to the diameter of a sphere of the same volume as the crystal measured. The instrument was calibrated with standard latex spheres (13.3 μm diameter). The samples, taken from the precipitation system 20 min after mixing the reactant solutions, were filtered, dried and then re-dispersed in 0.1 $mol\,dm^{-3}$ calcium chloride solution and measured immediately. The precipitate composition was characterized by a combination of FT-IR spectroscopic (Mattson), X-ray powder diffraction, XRD (Philips 1710), thermogravimetric (Mettler TG 50 thermobalance with a TC 11 TA processor) and SEM (Philips XL20) analyses, and the specific surface area of the crystals was determined by the multiple BET method (Micromeritics) using nitrogen. The total content of calcium and magnesium ions in the solid phase was determined by ion chromatography. The extent of isomorphic substitution of magnesium for calcium in the calcite structure was evaluated by measuring the calcite unit cell parameter by XRD.

Apart from XRD, the possible incorporation of foreign cations and anions into the crystal structure of calcite was also studied by EPR spectroscopy (Varian E-9 spectrometer equipped with a dual microwave resonant cavity). To study the local environment of Ca^{2+} in the crystal lattice of calcite, Mn^{2+} ions were used as a paramagnetic substitute for Ca^{2+} and were doped into the calcite structure. For this purpose, Mn^{2+} was added at a concentration of $2.0\times10^{-7}\ mol\,dm^{-3}$ to the carbonic acid solution before mixing the reactants, so that the manganese substitution for calcium took place during the precipitation of calcium carbonate.[18] Pure calcite crystals, the EPR spectrum of which was used as a reference, were prepared by adding 500 cm^3 of $2.0\times10^{-2}\ mol\,dm^{-3}$ calcium chloride solution to an equal volume of sodium carbonate solution of the same concentration. After the initial mixing of the reactants, the system was agitated mechanically with a flat-bladed stirrer for 3 h at a constant rate, and then aged for 24 h without further stirring. The calcite thus obtained was filtered, dried and stored in a desiccator.

The EPR spectra of all powder samples were measured and a qualitative interpretation of the spectral parameters proposed by Angus et al.[19] was applied. These authors reported that the axial distortion parameter D' of the calcite unit cell depended on temperature, pressure and the concentration and nature of the impurity ions incorporated into calcite. In the magnetic field and in the absence of any ligands, Mn^{2+} ions give six lines in the EPR spectrum due to the hyperfine interaction of the high electron spin state, $S = {}^5/_2$, with the nuclear spin of $^{55}Mn^{2+}$ nuclei, $I = {}^5/_2$. The crystal field of the CO_3^{2-} ligands in the calcite unit cell splits these spectral lines further, giving rise to a multi-line EPR spectrum (Figure 9b)which provides information on the CO_3^{2-} symmetry of the calcite lattice. Any axial distortion of the CO_3^{2-} ligands around Mn^{2+} in the calcite lattice (Figure 9a, double-ended arrows) changes parameter D' in the spectrum (Figure 9b, inset). This parameter is best regarded as a measure of the separation of the parallel and perpendicular components of each of the six main hyperfine lines in the EPR spectra of calcite and is high-

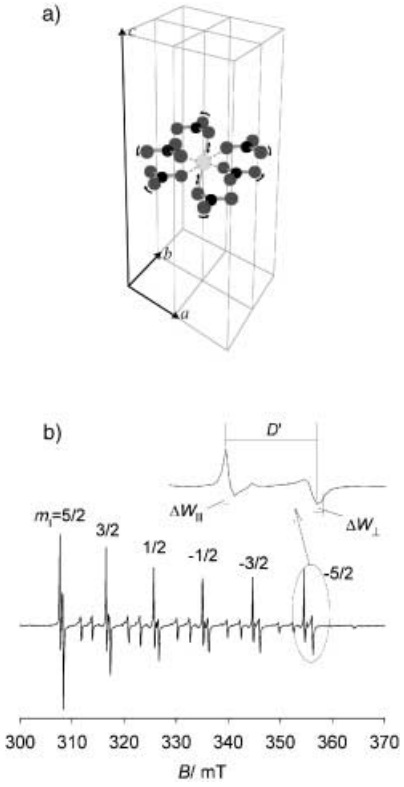

Figure 9. a) Environment of CO_3^{2-} groups around a Mn^{2+} ion substituted for Ca^{2+} in the calcite lattice. b) The six main hyperfine lines; inset: expansion of the $m_{Mn} = -{}^5/_2$ line and the wing lines, showing the definition of the measured parameters. Double-ended arrows indicate the possible axial distortions along the c axis; simple arrows denote the random displacements of CO_3^{2-} groups around their equilibrium positions.

est for the hyperfine line $m_{Mn} = -5/2$ (Figure 9b, inset). The lineshapes ΔW (Figure 9b, inset) of the Mn^{2+} spectra are expected to be Lorenzian because of homogeneous line-broadening. Deviations from these ideal lineshapes (Figure 9b), giving rise to an inhomogeneous line-broadening, can be caused by many effects. As suggested by Barberis et al.,[23] a random distribution of oxygen atoms of the CO_3^{2-} groups about their equilibrium positions in the calcite lattice (Figure 9a, simple arrows) can be induced by the impurity ions. In the EPR spectra, this is reflected as broadening of all the spectral lines and measured by the parallel ($\Delta W_{\parallel}$) and perpendicular ($\Delta W_{\perp}$) linewidths of the hyperfine line $m_{Mn} = -5/2$ at half-height from the baseline.

Acknowledgements

We thank Mr. Krunoslav Mirosavljević, B.Sc., for the EPR spectra. This research has been supported by the Ministry of Science and Technology of the Republic of Croatia (Project No. 0098061).

[1] Lj. Brečević, A. E. Nielsen, *J. Cryst. Growth* **1989**, *98*, 504–510.
[2] L. Addadi, S. Raz, S. Weiner, *Adv. Mater.* **2003**, *15*, 959–970.
[3] W. M. Jung, S. H. Kang, W.-S. Kim, C. K. Choi, *Chem. Eng. Sci.* **2000**, *49(55)*, 733–747.
[4] J. García-Carmona, J. Gómez-Morales, R. Rodrígez-Clemente, *J. Colloid Interface Sci.* **2003**, *261*, 434–440.
[5] S. Weiner, L. Addadi, *J. Mater. Chem.* **1997**, *7*, 689–702.
[6] G. Falini, *Int. J. Inorg. Mater.* **2000**, *2*, 455–461.
[7] S. Mann, *Biomineralization: Principles and Concepts in Bioinorganic Materials Chemistry*, Oxford University Press, Oxford, **2001**.
[8] H. Cölfen, *Curr. Opin. Colloid Interface Sci.* **2003**, *8*, 23–31.
[9] G. Falini, M. Gazzano, A. Ripamonti, *J. Cryst. Growth* **1994**, *137*, 577–584.
[10] F. C. Meldrum, S. T. Hyde, *J. Cryst. Growth* **2001**, *231*, 544–558.
[11] G. Falini, M. Gazzano, A. Ripamonti, *Chem. Commun.* **1996**, 1037–1038.
[12] K. J. Davis, P. M. Dove, J. J. De Yoreo, *Science* **2000**, *290*, 1134–1137.
[13] F. Manoli, E. Dalas, *J. Cryst. Growth* **2000**, *218*, 359–364.
[14] O. S. Pokrovsky, *J. Cryst. Growth* **1998**, *186*, 233–239.
[15] H. Cölfen, L. Qi, *Chem. Eur. J.* **2001**, *7*, 106–116.
[16] Y.- J. Han, J. Aizenberg, *J. Am. Chem. Soc.* **2003**, *125*, 4032–4033.
[17] Y. Kitano, *Bull. Chem. Soc. Jpn.* **1962**, *35*, 1973–1980.
[18] Lj. Brečević, V. Nöthig-Laslo, D. Kralj, S. Popović, *J. Chem. Soc. Faraday Trans.* **1996**, *92*, 1017–1022.
[19] J. G. Angus, J. B. Raynor, M. Robson, *Chem. Geol.* **1979**, *27*, 181–205.
[20] F. K. Hurd, M. Suchs, W. D. Hershberger, *Phys. Rev.* **1954**, *93*, 373–380.
[21] H. M. McConnell, *J. Chem. Phys.* **1956**, *24*, 904–905.
[22] C. Kikuchi, L. M. Matarrese, *J. Chem. Phys.* **1960**, *33*, 601–606.
[23] G. Barberis, R. Calvo, H. G. Maldonado, C. E. Zarate, *Phys. Rev. B* **1975**, *12*, 853–860.
[24] D. J. J. Kinsman, H. D. Holland, *Geochim. Cosmochim. Acta* **1969**, *33*, 1–17.
[25] D. Kralj, Lj. Brečević, J. Kontrec, *J. Cryst. Growth* **1997**, *177*, 248–257.
[26] D. Kralj, Lj. Brečević, A. E. Nielsen, *J. Cryst. Growth* **1990**, *104*, 793–800.
[27] D. Kralj, Lj. Brečević, A. E. Nielsen, *J. Cryst. Growth* **1994**, *143*, 269–276.
[28] A. E. Nielsen, J. M. Toft, *J. Cryst. Growth* **1984**, *67*, 278–288.
[29] M. Kitamura, *J. Colloid Interface Sci.* **2001**, *236*, 318–327.
[30] F. A. Andersen, Lj. Brečević, *Acta Chem. Scand.* **1991**, *45*, 1018–1024.
[31] S. Raz, S. Weiner, L. Addadi, *Adv. Mater.* **2000**, *12*, 38–42.
[32] E. Loste, R. M. Wilson, R. Seshardi, F. C. Meldrum, *J. Cryst. Growth* **2003**, *254*, 206–218.
[33] F. A. Andersen, D. Kralj, *Appl. Spectrosc.* **1991**, *45*, 1748–1751.
[34] S. Raz, P. C. Hamilton, F. H. Wilt, S. Weiner, L. Addadi, *Adv.Funct. Mater.* **2003**, *13*, 480–486.
[35] V. Nöthig-Laslo, Lj. Brečević, *J. Chem. Soc. Faraday Trans.* **1998**, *94*, 2005–2009.
[36] P. Moller , G. Rajagopalan, *Z. Phys. Chem. (München)* **1975**, *94*, 297–314.
[37] M. Kitamura, H. Konno, A. Yasui, H. Masuoka, *J. Cryst. Growth* **2002**, *236*, 323–332.
[38] R. Goldsmith, D. L. Graf, H. L. Heard, *North Am. Miner. News Am.* **1961**, *46*, 453–457.
[39] M. C. Van der Leeden, G. M. Van Rosmalen, *Desalination* **1987**, *66*, 185–200.
[40] M. Prieto, A. Putnis, L. Fernández-Díaz, S. López-Andrés, *J. Cryst. Growth* **1994**, *142*, 225–235.
[41] J. O. Titiloye, S. C. Parker, S. Mann, *J. Cryst. Growth* **1993**, *131*, 533–545.
[42] S. L. Tracy, C. J. P. François, H. M. Jennings, *J. Cryst. Growth* **1998**, *193*, 374–381.

Received: July 8, 2003
Revised: December 1, 2003 [F5313]